



HAL
open science

A Multilevel Schwarz Preconditioner Based on a Hierarchy of Robust Coarse Spaces

Hussam Al Daas, Laura Grigori, Pierre Jolivet, Pierre-Henri Tournier

► **To cite this version:**

Hussam Al Daas, Laura Grigori, Pierre Jolivet, Pierre-Henri Tournier. A Multilevel Schwarz Preconditioner Based on a Hierarchy of Robust Coarse Spaces. *SIAM Journal on Scientific Computing*, 2021, 43 (3), pp.A1907-A1928. 10.1137/19M1266964 . hal-02151184v2

HAL Id: hal-02151184

<https://hal.science/hal-02151184v2>

Submitted on 7 Dec 2020

HAL is a multi-disciplinary open access archive for the deposit and dissemination of scientific research documents, whether they are published or not. The documents may come from teaching and research institutions in France or abroad, or from public or private research centers.

L'archive ouverte pluridisciplinaire **HAL**, est destinée au dépôt et à la diffusion de documents scientifiques de niveau recherche, publiés ou non, émanant des établissements d'enseignement et de recherche français ou étrangers, des laboratoires publics ou privés.

A MULTILEVEL SCHWARZ PRECONDITIONER BASED ON A HIERARCHY OF ROBUST COARSE SPACES*

HUSSAM AL DAAS[†], LAURA GRIGORI[†], PIERRE JOLIVET[‡], AND PIERRE-HENRI
TOURNIER[§]

Abstract. In this paper we present a multilevel preconditioner based on overlapping Schwarz methods for symmetric positive definite (SPD) matrices. Robust two-level Schwarz preconditioners exist in the literature to guarantee fast convergence of Krylov methods. As long as the dimension of the coarse space is reasonable, that is, exact solvers can be used efficiently, two-level methods scale well on parallel architectures. However, the factorization of the coarse space matrix may become costly at scale. An alternative is then to use an iterative method on the second level, combined with an algebraic preconditioner, such as a one-level additive Schwarz preconditioner. Nevertheless, the condition number of the resulting preconditioned coarse space matrix may still be large. One of the difficulties of using more advanced methods, like algebraic multigrid or even two-level overlapping Schwarz methods, to solve the coarse problem is that the matrix does not arise from a partial differential equation (PDE) anymore. We introduce in this paper a robust multilevel additive Schwarz preconditioner where at each level the condition number is bounded, ensuring a fast convergence for each nested solver. Furthermore, our construction does not require any additional information than for building a two-level method, and may thus be seen as an algebraic extension.

Key words. domain decomposition, multilevel, elliptic problems, subspace correction

AMS subject classifications. 65F08, 65F10, 65N55

1. Introduction. We consider the solution of a linear system of equations

$$(1.1) \quad Ax = b,$$

where $A \in \mathbb{R}^{n \times n}$ is a symmetric positive definite (SPD) matrix, $b \in \mathbb{R}^n$ is the right-hand side, and $x \in \mathbb{R}^n$ is the vector of unknowns. To enhance convergence, it is common to solve the preconditioned system

$$M^{-1}Ax = M^{-1}b.$$

Standard domain decomposition preconditioners such as block Jacobi, additive Schwarz, and restricted additive Schwarz methods are widely used [32, 9, 8]. In a parallel framework, such preconditioners have the advantage of relatively low communication costs. However, their role in lowering the condition number of the system typically deteriorates when the number of subdomains increases. Multilevel approaches have shown a large impact on enhancing the convergence of Krylov methods [33, 12, 7, 25, 20, 10, 21, 1, 15, 23, 34, 30]. In multigrid and domain decomposition communities, multilevel methods have proven their capacity of scaling up to large numbers of processors and tackling ill-conditioned systems [37, 4, 19]. While some preconditioners are purely algebraic [7, 20, 10, 26, 29, 16, 1], several multilevel methods are based on hierarchical meshing in both multigrid and domain decomposition communities [35, 9, 25, 15, 23]. Mesh coarsening depends on the geometry of the problem. One has to be careful when choosing a hierarchical structure since it can

*Submitted to the editors June 7, 2019.

[†]ALPINES, INRIA, Paris, France (aldaas.hussam@gmail.com, laura.grigori@inria.fr).

[‡]IRIT, CNRS, Toulouse, France (pierre.jolivet@enseeiht.fr).

[§]LJLL, CNRS, Paris, France (tournier@ljl.math.upmc.fr).

40 have a significant impact on the iteration count [23, 25]. In [23], the authors propose
 41 a multilevel Schwarz domain decomposition solver for the elasticity problem. Based
 42 on a heuristic approach and following the maximum independent set method [2], they
 43 coarsen the fine mesh while preserving the boundary in order to obtain a two-level
 44 method. This strategy is repeated recursively to build several levels. However, they
 45 do not provide a bound on the condition number of the preconditioned matrix of the
 46 multilevel method. Multilevel domain decomposition methods are mostly based on
 47 non-overlapping approaches [35, 9, 25, 23, 37, 4, 30, 34]. Two-level overlapping domain
 48 decomposition methods are well studied and provide robust convergence estimates
 49 [33, 12, 5]. However, extending such a construction to more than two levels while
 50 preserving robustness is not straightforward. In [6], the authors propose an algebraic
 51 multilevel additive Schwarz method. Their approach is inspired by algebraic multigrid
 52 strategies. One drawback of it is that it is sensitive to the number of subdomains. In
 53 [15], the authors suggest applying the two-level Generalized Dryja–Smith–Widlund
 54 preconditioner recursively to build a multilevel method. In this case, the condition
 55 number bound of the two-level approach depends on the width of the overlap, the
 56 diameter of discretization elements, and the diameter of the subdomains. They focus
 57 on the preconditioner for the three-level case. One drawback of their approach is that
 58 the three-level preconditioner requires more iterations than the two-level variant. In
 59 this paper, the only information from the PDE needed for the construction of the
 60 preconditioner consists of the local Neumann matrices at the fine level. These ma-
 61 trices correspond to the integration of the bilinear form in the weak formulation of
 62 the studied PDE on the subdomain-decomposed input mesh. No further information
 63 is necessary: except on the fine level, our method is algebraic and does not depend
 64 on any coarsened mesh or auxiliary discretized operator. For problems not arising
 65 from PDE discretization, one needs to supply the local SPSD matrices on the finest
 66 level. In [3], a subset of the authors propose a fully algebraic approximation for such
 67 matrices. However, their approximation strategy is heuristic and may not be effective
 68 in some cases.

69 Our preconditioner is based on a hierarchy of coarse spaces and is defined as fol-
 70 lowing. At the first level, the set of unknowns is partitioned into N_1 subdomains and
 71 each subdomain has an associated matrix $A_{1,j} = R_{1,j}AR_{1,j}^\top$ obtained by using appro-
 72 priate restriction and prolongation operators $R_{1,j}$ and $R_{1,j}^\top$ respectively, defined in the
 73 following section. The preconditioner is formed as an additive Schwarz preconditioner
 74 coupled with an additive coarse space correction, defined as,

$$75 \quad M^{-1} = M_1^{-1} = V_1A_2^{-1}V_1^\top + \sum_{j=1}^{N_1} R_{1,j}^\top A_{1,j}^{-1} R_{1,j},$$

76 where V_1 is a tall-and-skinny matrix spanning a coarse space obtained by solving for
 77 each subdomain $j = 1$ to N_1 a generalized eigenvalue problem involving the matrix
 78 $A_{1,j}$ and the Neumann matrix associated with subdomain j . The coarse space matrix
 79 is $A_2 = V_1^\top AV_1$. This is equivalent to the GenEO preconditioner, and is described
 80 in detail in [33] and recalled briefly in section 2. The dimension of the coarse space
 81 is proportional to the number of subdomains N_1 . When it increases, factorizing A_2
 82 by using a direct method becomes prohibitive, and hence the application of A_2^{-1} to a
 83 vector should also be performed through an iterative method.

84 Our multilevel approach defines a hierarchy of coarse spaces V_i and coarse space
 85 matrices A_i for $i = 2$ to any depth $L + 1$, and defines a preconditioner M_i^{-1} such that
 86 the condition number of $M_i^{-1}A_i$ is bounded. The depth $L + 1$ is chosen such that the

87 coarse space matrix A_{L+1} can be factorized efficiently by using a direct method. At
 88 each level i , the graph of the coarse space matrix A_i is partitioned into N_i subdomains,
 89 and each subdomain j is associated with a local matrix $A_{i,j} = R_{i,j}A_iR_{i,j}^\top$ obtained by
 90 using appropriate restriction and prolongation operators $R_{i,j}$ and $R_{i,j}^\top$, respectively.
 91 The preconditioner at level i is defined as,

$$92 \quad M_i^{-1} = V_i A_{i+1}^{-1} V_i^\top + \sum_{j=1}^{N_i} R_{i,j}^\top A_{i,j}^{-1} R_{i,j},$$

93 where the coarse space matrix is $A_{i+1} = V_i^\top A_i V_i$.

94 One of the main contributions of the paper concerns the construction of the
 95 hierarchy of coarse spaces V_i for levels i going from 2 to L , that are built algebraically
 96 from the coarse space of the previous level V_{i-1} . This construction is based on the
 97 definition of local symmetric positive semi-definite (SPSD) matrices associated with
 98 each subdomain j at each level i that we introduce in this paper. These matrices are
 99 obtained by using the local SPSP matrices of the previous level $i-1$ and the previous
 100 coarse space V_{i-1} . They are then involved, with the local matrices $A_{i,j}$, in concurrent
 101 generalized eigenvalue problems solved for each subdomain j that allows to compute
 102 the local eigenvectors contributing to the coarse space V_i .

103 We show in [Theorem 5.3, section 5](#), that the condition number of $M_i^{-1}A_i$ is
 104 bounded and depends on the maximum number of subdomains at the first level that
 105 share an unknown, the number of distinct colors required to color the graph of A_i so
 106 that $\{span\{R_{i,j}^\top\}\}_{1 \leq j \leq N_i}$ of the same color are mutually A_i -orthogonal, and a user
 107 defined tolerance τ . It is thus independent of the number of subdomains N_i .

108 The main contribution of this paper is based on the combination of two previous
 109 works on two-level additive Schwarz methods [\[3, 33\]](#). The coarse space proposed in
 110 [\[33\]](#) guarantees an upper bound on the condition number that can be prescribed by
 111 the user. The SPSP splitting in the context of domain decomposition presented in
 112 [\[3\]](#) provides an algebraic view for the construction of coarse spaces. The combination
 113 of these two works leads to a robust multilevel additive Schwarz method. Here,
 114 robustness refers to the fact that at each level, an upper bound on the condition
 115 number of the associated matrix can be prescribed by the user a priori. The rest
 116 of the paper is organized as follows. In the next section, we present the notations
 117 used throughout the paper. In [section 2](#), we present a brief review of the theory of
 118 one- and two-level additive Schwarz methods. We extend in [section 3](#) the class of
 119 SPSP splitting matrices presented in [\[3\]](#) in order to make it suitable for multilevel
 120 methods. Afterwards, we define the coarse space at level i based on the extended
 121 class of local SPSP splitting matrices associated with this level. [Section 4](#) describes
 122 the partitioning of the domain at level $i+1$ from the partitioning at level i . In
 123 [Section 5](#), we explain the computation of the local SPSP matrices associated with each
 124 subdomain at level $i+1$. We compute them using those associated with subdomains
 125 at level i . [Section 6](#) presents numerical experiments on highly challenging diffusion
 126 and linear elasticity problems in two- and three-dimensional problems. We illustrate
 127 the theoretical robustness and practical usage of our proposed method by performing
 128 strong scalability tests up to 8,192 processes.

129 **Context and notation.** By convention, the finest level, on which [\(1.1\)](#) is de-
 130 fined, is the first level. A subscript index is used in order to specify which level
 131 an entity is defined on. In the case where additional subscripts are used, the first
 132 subscript always denotes the level. For the sake of clarity, we omit the subscript cor-

133 responding to level 1 when it is clear from context, e.g., matrix A . Furthermore, the
 134 subscripts i and j always refer to a specific level i and its subdomain j , respectively.
 135 The number of levels is $L + 1$. Let $A_i \in \mathbb{R}^{n_i \times n_i}$ denote symmetric positive definite
 136 matrices, each corresponding to level $i = 1, \dots, L + 1$. We suppose that a direct solver
 137 can be used at level $L + 1$ to compute an exact factorization of A_{L+1} .

138 Let $B \in \mathbb{R}^{p \times q}$ be a matrix. Let $P \subset \llbracket 1; p \rrbracket$ and $Q \subset \llbracket 1; q \rrbracket$ be two sets of
 139 indices. The concatenation of P and Q is represented by $[P, Q]$. We note that the
 140 order of the concatenation is important. $B(P, \cdot)$ is the submatrix of B formed by
 141 the rows whose indices belong to P . $B(\cdot, Q)$ is the submatrix of B formed by the
 142 columns whose indices belong to Q . $B(P, Q) = (B(P, \cdot))(\cdot, Q)$. The identity matrix
 143 of size p is denoted I_p . We suppose that the graph of A_i is partitioned into N_i non-
 144 overlapping subdomains, where $N_i \ll n_i$ and $N_{i+1} \leq N_i$ for $i = 1, \dots, L$. We note that
 145 partitioning at level 1 can be performed by using a graph partitioning library such as
 146 ParMETIS [22] or PT-SCOTCH [11]. Partitioning at greater levels will be described
 147 later in section 4. In the following, we define for each level $i = 1, \dots, L$ notations
 148 for subsets and restriction operators that are associated with the partitioning. Let
 149 $\Omega_i = \llbracket 1; n_i \rrbracket$ be the set of unknowns at level i and let $\Omega_{i,j,I}$ for $j = 1, \dots, N_i$ be the
 150 subset of Ω_i that represents the unknowns in subdomain j . We refer to $\Omega_{i,j,I}$ as the
 151 *interior unknowns* of subdomain j . Let $\Gamma_{i,j}$ for $j = 1, \dots, N_i$ be the subset of Ω_i that
 152 represents the neighbor unknowns of subdomain j , i.e., the unknowns at distance 1
 153 from subdomain j through the graph of A_i . We refer to $\Gamma_{i,j}$ as the *overlapping*
 154 *unknowns* of subdomain j . We denote $\Omega_{i,j} = [\Omega_{i,j,I}, \Gamma_{i,j}]$, for $j = 1, \dots, N_i$, the
 155 concatenation of interior and overlapping unknowns of subdomain j . We denote
 156 $\Delta_{i,j}$, for $j = 1, \dots, N_i$, the complementary of $\Omega_{i,j}$ in Ω_i , i.e., $\Delta_{i,j} = \Omega_i \setminus \Omega_{i,j}$. In
 157 Figure 1.1, a triangular mesh is used to discretize a square domain. The set of
 158 nodes of the mesh is partitioned into 16 disjoint subsets $\Omega_{1,j,I}$, which represent a
 159 non-overlapping decomposition, for $j = 1, \dots, 16$ (left). On the left, a matrix A_1
 160 whose connectivity graph corresponds to the mesh is illustrated. The submatrix
 161 $A_1(\Omega_{1,j,I}, \Omega_{1,j,I})$ is associated with the non-overlapping subdomain j . Each submatrix
 162 $A_1(\Omega_{1,j,I}, \Omega_{1,j,I})$ is colored with a distinct color. The same color is used to color the
 163 region that contains the nodes in the non-overlapping subdomain $\Omega_{1,j,I}$. Note that
 164 if two subdomains j_1, j_2 are neighbors, the submatrix $A_1(\Omega_{1,j_1,I}, \Omega_{1,j_2,I})$ has nonzero
 165 elements. For $j = 1, \dots, N_i$, we denote by $n_{i,j,I}$, $\gamma_{i,j}$ and $n_{i,j}$ the cardinality of $\Omega_{i,j,I}$,
 166 $\Gamma_{i,j}$ and $\Omega_{i,j}$ respectively.

167 Let $R_{i,j,I} \in \mathbb{R}^{n_{i,j,I} \times n_i}$ be defined as $R_{i,j,I} = I_{n_i}(\Omega_{i,j,I}, \cdot)$.

168 Let $R_{i,j,\Gamma} \in \mathbb{R}^{\gamma_{i,j} \times n_i}$ be defined as $R_{i,j,\Gamma} = I_{n_i}(\Gamma_{i,j}, \cdot)$.

169 Let $R_{i,j} \in \mathbb{R}^{n_{i,j} \times n_i}$ be defined as $R_{i,j} = I_{n_i}(\Omega_{i,j}, \cdot)$.

170 Let $R_{i,j,\Delta} \in \mathbb{R}^{(n_i - n_{i,j}) \times n_i}$ be defined as $R_{i,j,\Delta} = I_{n_i}(\Delta_{i,j}, \cdot)$.

171 Let $\mathcal{P}_{i,j} = I_{n_i}([\Omega_{i,j,I}, \Gamma_{i,j}, \Delta_{i,j}], \cdot) \in \mathbb{R}^{n_i \times n_i}$, be a permutation matrix associated
 172 with the subdomain j , for $j = 1, \dots, N_i$. The matrix of the overlapping subdomain j ,
 173 $R_{i,j} A_i R_{i,j}^\top$, is denoted $A_{i,j}$. We denote $D_{i,j} \in \mathbb{R}^{n_{i,j} \times n_{i,j}}$, $j = 1, \dots, N_i$, any set of
 174 non-negative diagonal matrices such that

$$175 \quad I_{n_i} = \sum_{j=1}^{N_i} R_{i,j}^\top D_{i,j} R_{i,j}.$$

176 We refer to $\{D_{i,j}\}_{1 \leq j \leq N_i}$ as the algebraic partition of unity. Let $V_i \in \mathbb{R}^{n_i \times n_{i+1}}$ be
 177 a tall-and-skinny matrix of full rank. We denote \mathcal{S}_i the subspace spanned by the
 178 columns of V_i . This subspace will stand for the coarse space associated with level i .
 179 By convention, we refer to \mathcal{S}_i as subdomain 0 at level i . Thus, we have $n_{i,0} = n_{i+1}$.

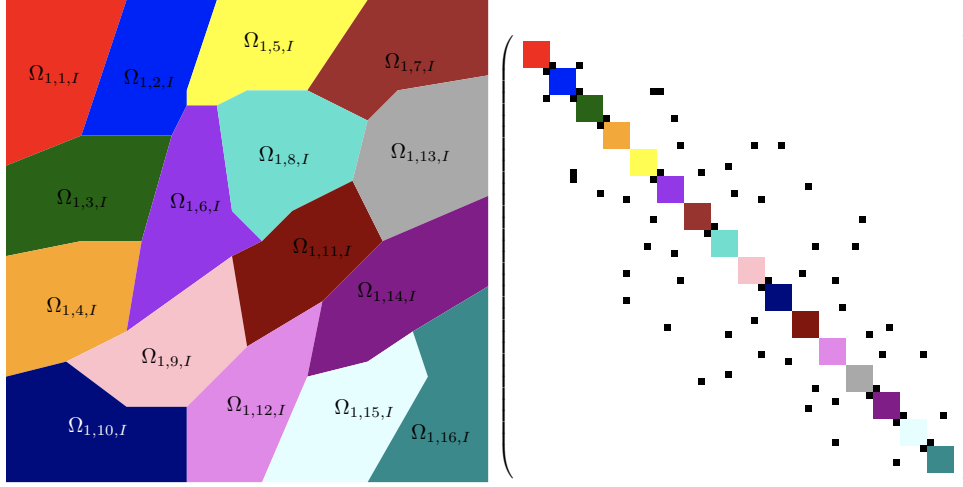


FIG. 1.1. *Left: a triangular mesh is used to discretize the unit square. The set of nodes of the mesh is partitioned into 16 disjoint subsets, non-overlapping subdomains, $\Omega_{1,j,I}$ for $j = 1, \dots, 16$. Right: Illustration of the matrix A_1 whose connectivity graph corresponds to the mesh on the left. The diagonal block j of A_1 corresponds to the non-overlapping subdomain $\Omega_{1,j,I}$. Each submatrix $A_1(\Omega_{1,j,I}, \Omega_{1,j,I})$ is colored with a distinct color. The same color is used to color the region of the square that contains nodes in $\Omega_{1,j,I}$.*

180 The interpolation operator at level i is defined as:

$$\begin{aligned}
 & \mathcal{R}_{i,2}: \prod_{j=0}^{N_i} \mathbb{R}^{n_{i,j}} \rightarrow \mathbb{R}^{n_i} \\
 & (u_j)_{0 \leq j \leq N_i} \mapsto \sum_{j=0}^{N_i} R_{i,j}^\top u_j.
 \end{aligned}
 \tag{1.2}$$

183 Finally, we denote $\mathcal{V}_{i,j}$ the set of neighboring subdomains of each subdomain j at
 184 level i for $(i, j) \in \llbracket 1; L \rrbracket \times \llbracket 1; N_i \rrbracket$.

$$\mathcal{V}_{i,j} = \{k \in \llbracket 1; N_i \rrbracket : \Omega_{i,j} \cap \Omega_{i,k} \neq \emptyset\}.$$

186 As previously mentioned, partitioning at level 1 can be performed by graph parti-
 187 tioning libraries such as ParMETIS [22] or PT-SCOTCH [11]. Partitioning at further
 188 levels will be defined later: the sets $\Omega_{i,j,I}$, $\Omega_{i,j,\Gamma}$, $\Omega_{i,j}$, and $\Delta_{i,j}$ for $i > 1$ are defined
 189 in subsection 4.2. The coarse spaces \mathcal{S}_i as well as the projection and prolongation
 190 operators V_i^\top and V_i are defined in subsection 3.2. We suppose that the connectivity
 191 graph between the subdomains on each level is sparse. This assumption is not true in
 192 general, however, it is valid in structures based on locally constructed coarse spaces
 193 in domain decomposition as we show in this paper, see [18, Section 4.1 p.81] for the
 194 case of two levels.

195 **2. Background.** In this section, we review briefly several theoretical results
 196 related to additive Schwarz preconditioners. We introduce them for the sake of com-
 197 pleteness.

198 LEMMA 2.1 (fictitious subspace lemma). *Let $A \in \mathbb{R}^{n_A \times n_A}$, $B \in \mathbb{R}^{n_B \times n_B}$ be two*

199 symmetric positive definite matrices. Let \mathcal{R} be an operator defined as

$$\begin{aligned} 200 \quad & \mathcal{R}: \mathbb{R}^{n_B} \rightarrow \mathbb{R}^{n_A} \\ 201 \quad & v \mapsto \mathcal{R}v, \end{aligned}$$

202 and let \mathcal{R}^\top be its transpose. Suppose that the following conditions hold:

- 203 1. The operator \mathcal{R} is surjective.
- 204 2. There exists $c_u > 0$ such that

$$205 \quad (\mathcal{R}v)^\top A (\mathcal{R}v) \leq c_u v^\top B v, \quad \forall v \in \mathbb{R}^{n_B}.$$

- 206 3. There exists $c_l > 0$ such that for all $v_{n_A} \in \mathbb{R}^{n_A}, \exists v_{n_B} \in \mathbb{R}^{n_B} | v_{n_A} = \mathcal{R}v_{n_B}$
- 207 and

$$208 \quad c_l v_{n_B}^\top B v_{n_B} \leq (\mathcal{R}v_{n_B})^\top A (\mathcal{R}v_{n_B}) = v_{n_A}^\top A v_{n_A}.$$

209 Then, the spectrum of the operator $\mathcal{R}B^{-1}\mathcal{R}^\top A$ is contained in the segment $[c_l, c_u]$.

210 *Proof.* We refer the reader to [12, Lemma 7.4 p.164] or [28, 27, 13] for a detailed
211 proof. \square

212 LEMMA 2.2. The operator $\mathcal{R}_{i,2}$ as defined in (1.2) is surjective.

213 *Proof.* The proof follows from the definition of $\mathcal{R}_{i,2}$ (1.2). \square

214 LEMMA 2.3. Let $k_{i,c}$ for $i = 1, \dots, L$ be the minimum number of distinct colors
215 so that $\{\text{span}\{R_{i,j}^\top\}\}_{1 \leq j \leq N_i}$ of the same color are mutually A_i -orthogonal. Then, we
216 have

$$\begin{aligned} 218 \quad & (\mathcal{R}_{i,2}u_{\mathcal{B}_i})^\top A_i (\mathcal{R}_{i,2}u_{\mathcal{B}_i}) \\ 219 \quad & \leq (k_{i,c} + 1) \sum_{j=0}^{N_i} u_j^\top (R_{i,j} A_i R_{i,j}^\top) u_j, \quad \forall u_{\mathcal{B}_i} = (u_j)_{0 \leq j \leq N_i} \in \prod_{j=0}^{N_i} \mathbb{R}^{n_{i,j}}. \end{aligned}$$

221 *Proof.* We refer the reader to [9, Theorem 12 p.93] for a detailed proof. \square

222 We note that at level i , the number $k_{i,c}$ is smaller than the maximum number of
223 neighbors over the set of subdomains $\llbracket 1; N_i \rrbracket$

$$224 \quad k_{i,c} \leq \max_{1 \leq j \leq N_i} \#\mathcal{V}_{i,j}.$$

225 Due to the sparse structure of the connectivity graph between the subdomains at
226 level i , the maximum number of neighbors over the set of subdomains $\llbracket 1; N_i \rrbracket$ is
227 independent of the number of subdomains N_i . Then, so is $k_{i,c}$.

228 LEMMA 2.4. Let $u_{A_i} \in \mathbb{R}^{n_{A_i}}$ and $u_{\mathcal{B}_i} = \{u_j\}_{0 \leq j \leq N_i} \in \prod_{j=0}^{N_i} \mathbb{R}^{n_{i,j}}$ such that $u_{A_i} =$
229 $\mathcal{R}_{i,2}u_{\mathcal{B}_i}$. The additive Schwarz operator without any other restriction on the coarse
230 space \mathcal{S}_i verifies the following inequality

$$231 \quad \sum_{j=0}^{N_i} u_j^\top (R_{i,j} A_i R_{i,j}^\top) u_j \leq 2u_{A_i}^\top A_i u_{A_i} + (2k_{i,c} + 1) \sum_{j=1}^{N_i} u_j^\top R_{i,j} A_i R_{i,j}^\top u_j,$$

232 where $k_{i,c}$ is defined in Lemma 2.3.

233 *Proof.* We refer the reader to [12, Lemma 7.12, p. 175] to view the proof in
 234 detail. \square

235 **LEMMA 2.5.** *Let $A, B \in \mathbb{R}^{m \times m}$ be two symmetric positive semi-definite matrices.*
 236 *Let $\ker(A)$, $\text{range}(A)$ denote the null space and the range of A respectively. Let P_0*
 237 *be an orthogonal projection on $\text{range}(A)$. Let τ be a positive real number. Consider*
 238 *the generalized eigenvalue problem,*

$$239 \quad P_0 B P_0 u_k = \lambda_k A u_k,$$

$$240 \quad (u_k, \lambda_k) \in \text{range}(A) \times \mathbb{R}.$$

241 *Let P_τ be an orthogonal projection on the subspace*

$$242 \quad Z = \ker(A) \oplus \text{span}\{u_k | \lambda_k > \tau\},$$

243 *then, the following inequality holds:*

$$244 \quad (2.1) \quad (u - P_\tau u)^\top B (u - P_\tau u) \leq \tau u^\top A u, \quad \forall u \in \mathbb{R}^m.$$

245 *Proof.* We refer the reader to [3, Lemma 2.4] and [12, Lemma 7.7] for a detailed
 246 proof. \square

247 **2.1. GenEO coarse space.** In [33, 12] the authors present the GenEO coarse
 248 space which relies on defining appropriate symmetric positive semi-definite (SPSD)
 249 matrices $\tilde{A}_j \in \mathbb{R}^{n \times n}$ for $j = 1, \dots, N$. These are the unassembled Neumann matrices,
 250 corresponding to the integration on each subdomain of the operator defined in the
 251 variational form of the PDE. These matrices are local, i.e., $R_{j,\Delta} \tilde{A}_j = 0$. Furthermore,
 252 they verify the relations

$$u^\top \tilde{A}_j u \leq u^\top A u, \quad \forall u \in \mathbb{R}^n,$$

$$253 \quad u^\top \sum_{j=1}^N \tilde{A}_j u \leq k_{\text{GenEO}} u^\top A u, \quad \forall u \in \mathbb{R}^n,$$

254 where $k_{\text{GenEO}} \leq N$ is the maximum number of subdomains that share an unknown.

255 **2.2. Local SPSPD splitting of an SPD matrix.** In [3], the authors present
 256 the local SPSPD splitting of an SPD matrix. Given the permutation matrix \mathcal{P}_j , a local
 257 SPSPD splitting matrix \tilde{A}_j of A associated with subdomain j is defined as

$$259 \quad (2.2) \quad \mathcal{P}_j \tilde{A}_j \mathcal{P}_j^\top = \begin{pmatrix} R_{j,I} A R_{j,I}^\top & R_{j,I} A R_{j,\Gamma}^\top \\ R_{j,\Gamma} A R_{j,I}^\top & \tilde{A}_\Gamma^j \\ & & 0 \end{pmatrix},$$

260 where $\tilde{A}_\Gamma^j \in \mathbb{R}^{\gamma_j \times \gamma_j}$ satisfies the two following conditions: For all $u \in \mathbb{R}^{\gamma_j}$,

- 261 • $u^\top (R_{j,\Gamma} A R_{j,I}^\top) (R_{j,I} A R_{j,I}^\top)^{-1} (R_{j,I} A R_{j,\Gamma}^\top) u \leq u^\top \tilde{A}_\Gamma^j u$
- 262 • $u^\top \tilde{A}_\Gamma^j u \leq u^\top \left((R_{j,\Gamma} A R_{j,\Gamma}^\top) - (R_{j,\Gamma} A R_{j,\Delta}^\top) (R_{j,\Delta} A R_{j,\Delta}^\top)^{-1} (R_{j,\Delta} A R_{j,\Gamma}^\top) \right) u.$

263 The authors prove that the matrices \tilde{A}_j defined in such a way verify the following
 264 relations:

$$265 \quad (2.3) \quad R_{j,\Delta} \tilde{A}_j = 0,$$

$$266 \quad (2.4) \quad u^\top \tilde{A}_j u \leq u^\top A u, \quad \forall u \in \mathbb{R}^n,$$

$$267 \quad (2.5) \quad u^\top \sum_{j=1}^N \tilde{A}_j u \leq k u^\top A u, \quad \forall u \in \mathbb{R}^n,$$

268

269 where k is a number that depends on the local SPSD splitting matrices and can be
 270 at most equal to the number of subdomains $k \leq N$. The authors also show that the
 271 local matrices defined in GenEO [33, 12] can be seen as a local SPSD splitting.

272 In [3], the authors highlight that the key idea to construct a coarse space relies
 273 on the ability to identify the so-called local SPSD splitting matrices. They present
 274 a class of algebraically constructed coarse spaces based on the local SPSD splitting
 275 matrices. Moreover, this class can be extended to a larger variety of local SPSD
 276 matrices. This extension has the advantage of allowing to construct efficient coarse
 277 spaces for a multilevel structure in a practical way. This is discussed in the following
 278 section.

279 **3. Extension of the class of coarse spaces.** In this section we extend the
 280 class of coarse spaces presented in [3]. To do so, we present a class of matrices, that is
 281 larger than the class of local SPSD splitting matrices. This will be our main building
 282 block in the construction of efficient coarse spaces. Furthermore, this extension can
 283 lead to a straightforward construction of hierarchical coarse spaces in a multilevel
 284 Schwarz preconditioner setting.

285 **3.1. Extension of the class of local SPSD splitting matrices.** Regarding
 286 the two-level additive Schwarz method, the authors of [3] introduced the local SPSD
 287 splitting related to a subdomain as defined in (2.2). As it can be seen from the theory
 288 presented in that paper, it is not necessary to have the exact matrices $R_{j,I}AR_{j,I}^\top$,
 289 $R_{j,I}AR_{j,\Gamma}^\top$, and $R_{j,\Gamma}AR_{j,I}^\top$ in the definition of the local SPSD splitting in order to
 290 build an efficient coarse space. Indeed, the one and only necessary condition is to
 291 define for each subdomain j an SPSD matrix \tilde{A}_j for $j = 1, \dots, N$ such that:

$$292 \quad (3.1) \quad \begin{aligned} & R_{j,\Delta}\tilde{A}_j = 0, \\ & u^\top \sum_{j=1}^N \tilde{A}_j u \leq k u^\top A u, \forall u \in \mathbb{R}^n, \end{aligned}$$

294 where k is a number that depends on the local SPSD matrices \tilde{A}_j for $j = 1, \dots, N$.
 295 The first condition means that \tilde{A}_j has the local SPSD structure associated with sub-
 296 domain j , i.e., it has the following form:

$$297 \quad \mathcal{P}_j \tilde{A}_j \mathcal{P}_j^\top = \begin{pmatrix} \tilde{A}_{I,\Gamma}^j & 0 \\ 0 & 0 \end{pmatrix},$$

298 where $\tilde{A}_{I,\Gamma}^j \in \mathbb{R}^{n_j \times n_j}$. The second condition is associated with the stable decom-
 299 position property [36, 12]. Note that with regard to the local SPSD matrices, the
 300 authors in [33] only use these two conditions. That is to say, with matrices that verify
 301 conditions (3.1) the construction of the coarse space is straightforward through the
 302 theory presented in either [33] or [3]. To this end, we define in the following the local
 303 SPSD (LSPSD) matrix associated with subdomain j as well as the associated local
 304 filtering subspace that contributes to the coarse space.

305 **DEFINITION 3.1** (local SPSD matrices). *An SPSD matrix $\tilde{A}_{i,j} \in \mathbb{R}^{n_i \times n_i}$ is called*
 306 *local SPSD (LSPSD) with respect to subdomain j if*

- 307 • $R_{i,j,\Delta}\tilde{A}_{i,j} = 0$,
 - 308 • $u^\top \sum_{j=1}^{N_i} \tilde{A}_{i,j} u \leq k_i u^\top A_i u$,
- 309 where $k_i > 0$.

310 We note that the local SPSD splitting matrices form a subset of the local SPSD
 311 matrices.

312 **3.2. Multilevel coarse spaces.** This section summarizes the steps to be per-
 313 formed in order to construct the coarse space at level i once we have the LSPSD
 314 matrices associated with each subdomain at that level.

315 **DEFINITION 3.2** (coarse space based on LSPSD matrices). *Let $\tilde{A}_{i,j} \in \mathbb{R}^{n_i \times n_i}$ for*
 316 *$j = 1, \dots, N_i$ be LSPSD matrices. Let $D_{i,j} \in \mathbb{R}^{n_{i,j}}$ for $j = 1, \dots, N_i$ be the partition*
 317 *of unity. Let $\tau_i > 0$ be a given number. For a subdomain $j \in \llbracket 1; N_i \rrbracket$, let*

$$318 \quad G_{i,j} = D_{i,j} (R_{i,j} A_i R_{i,j}^\top) D_{i,j}.$$

319 *Let $\tilde{P}_{i,j}$ be the projection on $\text{range}(R_{i,j} \tilde{A}_j R_{i,j}^\top)$ parallel to $\ker(R_{i,j} \tilde{A}_j R_{i,j}^\top)$. Let $K_{i,j} =$*
 320 *$\ker(R_{i,j} \tilde{A}_{i,j} R_{i,j}^\top)$. Consider the generalized eigenvalue problem:*

$$321 \quad (3.2) \quad \begin{aligned} \tilde{P}_{i,j} G_{i,j} \tilde{P}_{i,j} u_{i,j,k} &= \lambda_{i,j,k} R_{i,j} \tilde{A}_{i,j} R_{i,j}^\top u_{i,j,k}, \\ (u_{i,j,k}, \lambda_{i,j,k}) &\in \text{range}(R_{i,j} \tilde{A}_{i,j} R_{i,j}^\top) \times \mathbb{R}. \end{aligned}$$

323 *Set*

$$324 \quad (3.3) \quad Z_{i,j} = K_{i,j} \oplus \text{span}\{u_{i,j,k} \mid \lambda_{i,j,k} > \tau_i\}.$$

325 *Then, the coarse space associated with LSPSD matrices $\tilde{A}_{i,j}$ for $j = 1, \dots, N_i$ at level i*
 326 *is defined as:*

$$327 \quad (3.4) \quad \mathcal{S}_i = \bigoplus_{j=1}^{N_i} R_{i,j}^\top D_{i,j} Z_{i,j}.$$

328 *Following notations from [section 1](#), the columns of V_i span the coarse space \mathcal{S}_i . The*
 329 *matrix A_{i+1} is defined as:*

$$330 \quad (3.5) \quad A_{i+1} = V_i^\top A_i V_i.$$

331 The local SPSD splitting matrices at level 1 will play an important role in the
 332 construction of the LSPSD matrices at subsequent levels. In the following, we present
 333 an efficient approach for computing LSPSD matrices for levels greater than 1.

334 **4. Partitioning for levels strictly greater than 1.** In this section, we ex-
 335 plain how to obtain the partitioning sets $\Omega_{i,j,I}$ for $(i,j) \in \llbracket 2; L \rrbracket \times \llbracket 1; N_i \rrbracket$. Once the
 336 sets $\Omega_{i,j,I}$ for $j = 1, \dots, N_i$ are defined at level i , the following elements are readily
 337 available: sets $\Gamma_{i,j}$, $\Delta_{i,j}$, and $\Omega_{i,j}$; restriction operators $R_{i,j,I}$, $R_{i,j,\Gamma}$, $R_{i,j,\Delta}$, and $R_{i,j}$;
 338 permutation matrices $\mathcal{P}_{i,j}$ for $j = 1, \dots, N_i$. The partition of unity is constructed in
 339 an algebraic way. The m th diagonal element of $D_{i,j}$ is 1 if $m \leq n_{i,j,I}$ and 0 otherwise.

340 **4.1. Superdomains as unions of several subdomains.** In this section, we
 341 introduce the notion of a *superdomain*. It refers to the union of several neighboring
 342 subdomains. Let $\mathcal{G}_{i,1}, \dots, \mathcal{G}_{i,N_{i+1}}$ be disjoint subsets of $\llbracket 1; N_i \rrbracket$, where $\bigcup_{j=1}^{N_{i+1}} \mathcal{G}_{i,j} =$
 343 $\llbracket 1; N_i \rrbracket$. We call the union of the subdomains $\{k \in \llbracket 1; N_i \rrbracket : k \in \mathcal{G}_{i,j}\}$ superdomain j ,
 344 for $j = 1, \dots, N_{i+1}$. [Figure 4.1](#) gives an example of how to set superdomains. Though
 345 this definition of superdomains may look somehow related to the fine mesh, it is in
 346 practice done at the algebraic level, as explained later on. Note that the indices of
 347 columns and rows of A_{i+1} are associated with the vectors contributed by the subdo-
 348 mains at level i in order to build the coarse space \mathcal{S}_i , see [Figure 4.2](#). Hence, defining
 349 subdomains on the structure of A_{i+1} is natural once we have the subsets $\mathcal{G}_{i,j}$, for
 350 $j = 1, \dots, N_{i+1}$.

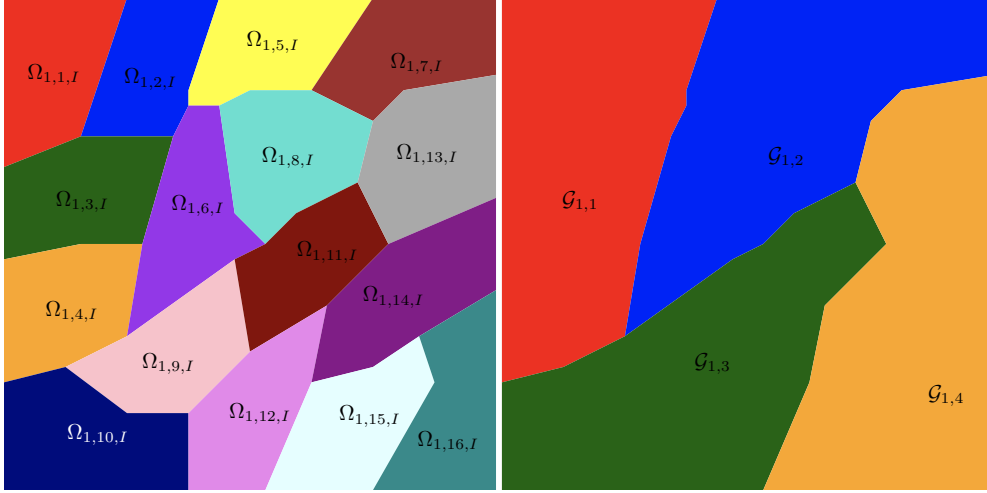


FIG. 4.1. Left: 16 subdomains at level 1. Right: 4 superdomains at level 1. $\mathcal{G}_{1,j} = \llbracket 4(j-1) + 1; 4(j-1) + 4 \rrbracket$.

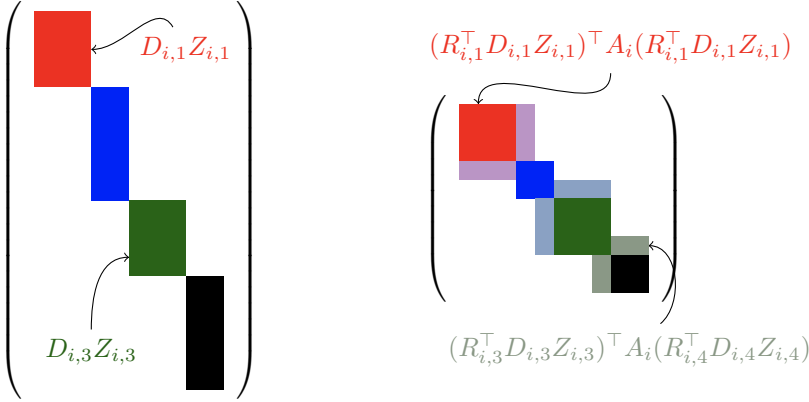


FIG. 4.2. Illustration of the correspondence of indices between the columns of V_i (left) and the rows and columns of A_{i+1} (right). Having no overlap in V_i is possible through a non-overlapping partition of unity.

351 **4.2. Heritage from superdomains.** Let $e_{i,j}$ be the set of indices of the vectors
 352 that span $R_{i,j}^\top D_{i,j} Z_{i,j}$ in the matrix V_i for some $(i, j) \in \llbracket 1; L-1 \rrbracket \times \llbracket 1; N_i \rrbracket$, see
 353 Figure 4.2. We define $\Omega_{i+1,j,I} = \cup_{k \in \mathcal{G}_{i,j}} e_{i,k}$, for $j = 1, \dots, N_{i+1}$. We denote $\Omega_{i+1,j,\Gamma}$
 354 the subset of $\llbracket 1; n_{i+1} \rrbracket \setminus \Omega_{i+1,j,I}$ whose elements are at distance 1 from $\Omega_{i+1,j,I}$ through
 355 the graph of A_{i+1} . We note that

$$356 \quad \Omega_{i+1,j,\Gamma} \subset \bigcup_{p \in \mathcal{G}_{i,j}} \bigcup_{k \in \mathcal{V}_{i,p}} e_{i,k},$$

357 where $\mathcal{V}_{i,j}$ represents the set of subdomains that are neighbors of subdomain j at
 358 level i for $j = 1, \dots, N_i$. The overlapping subdomain j is defined by the set $\Omega_{i+1,j} =$
 359 $[\Omega_{i+1,j,I}, \Omega_{i+1,j,\Gamma}]$. The rest of the sets, restriction, and prolongation operators can
 360 be defined as given in section 1.

361 **5. LSPSD matrices for levels strictly greater than 1.** In [33, 12, 3], differ-
 362 ent methods are suggested to obtain local SPSP splitting matrices at level 1. These
 363 matrices are used to construct efficient two-level additive Schwarz preconditioners.
 364 Here in this section, we do not discuss the construction of these matrices at level 1. We
 365 suppose that we have the local SPSP matrices $\tilde{A}_{1,j} \in \mathbb{R}^{n_1 \times n_1}$ for $j = 1, \dots, N_1$. We
 366 focus on computing LSPSD matrices $\tilde{A}_{i,j} \in \mathbb{R}^{n_i \times n_i}$ for $(i, j) \in \llbracket 2; L \rrbracket \times \llbracket 1; N_i \rrbracket$. We also
 367 suppose that the coarse space \mathcal{S}_1 is available, i.e., the matrices V_1 and $A_2 = V_1^\top A_1 V_1$
 368 are known explicitly.

369 **PROPOSITION 5.1.** *Let i be a fixed level index, and let $\tilde{A}_{i,j}$ be an LSPSD of A_i ,*
 370 *(see Definition 3.1), associated with subdomain j , for $j = 1, \dots, N_i$. Let $\mathcal{G}_{i,1}, \dots, \mathcal{G}_{i,N_{i+1}}$*
 371 *be a set of superdomains at level i associated with the partitioning at level $i + 1$, see*
 372 *subsection 4.1. Let V_i^\top be the restriction matrix to the coarse space at level i . Then,*
 373 *the matrix $\tilde{A}_{i+1,j}$ which is defined as:*

$$374 \quad \tilde{A}_{i+1,j} = \sum_{k \in \mathcal{G}_{i,j}} V_i^\top \tilde{A}_{i,k} V_i,$$

375 *satisfies the conditions in Definition 3.1. That is, $\tilde{A}_{i+1,j}$ is LSPSD of A_{i+1} with*
 376 *respect to subdomain j for $j = 1, \dots, N_{i+1}$.*

377 *Proof.* To prove that $\tilde{A}_{i+1,j}$ is LSPSD of A_{i+1} with respect to subdomain j , we
 378 have to prove the following:

- 379 • $R_{i+1,j,\Delta} \tilde{A}_{i+1,j} = 0$
- 380 • $u^\top \sum_{j=1}^{N_{i+1}} \tilde{A}_{i+1,j} u \leq k_{i+1} u^\top A_{i+1} u$ for all $u \in \mathbb{R}^{n_{i+1}}$.

381 First, note that $R_{i,k} \tilde{A}_{i,j} = 0$ for all non-neighboring subdomains k of subdomain j .
 382 This yields $Z_{i,k}^\top D_{i,k} R_{i,k} \tilde{A}_{i,j} = 0$ for these subdomains k .

383 Now, let $m \in \llbracket 1; n_{i+1} \rrbracket \setminus \Omega_{i+1,j}$. We will show that the m th row of $\tilde{A}_{i+1,j}$ is zero.
 384 Following the partitioning of subdomains at level $i + 1$, there exists a subdomain Ω_{p_0}
 385 such that the m th column of V_i is part of $R_{i,p_0}^\top D_{i,p_0} Z_{i,p_0}$. We denote this column
 386 vector by v_m . Furthermore, the subdomain p_0 is not a neighbor of any subdomain
 387 that is a part of the superdomain $\mathcal{G}_{i,j}$. Hence, $v_m^\top \tilde{A}_{i,k} = 0$ for $k \in \mathcal{G}_{i,j}$. The m th row
 388 of $\tilde{A}_{i+1,j}$ is given as $v_m^\top \sum_{k \in \mathcal{G}_{i,j}} \tilde{A}_{i,k} V_i$. Then, $v_m^\top \sum_{k \in \mathcal{G}_{i,j}} \tilde{A}_{i,k} = 0$, and the m th row
 389 of $\tilde{A}_{i+1,j}$ is zero.

390 To prove the second condition, we have

$$391 \quad u^\top \sum_{j=1}^{N_{i+1}} \tilde{A}_{i+1,j} u = u^\top \sum_{j=1}^{N_{i+1}} \sum_{k \in \mathcal{G}_{i,j}} V_i^\top \tilde{A}_{i,k} V_i u.$$

393 Since $\{\mathcal{G}_{i,j}\}_{1 \leq j \leq N_{i+1}}$ form a disjoint partitioning of $\llbracket 1; N_i \rrbracket$, we can write

$$394 \quad u^\top \sum_{j=1}^{N_{i+1}} \tilde{A}_{i+1,j} u = u^\top \sum_{k=1}^{N_i} V_i^\top \tilde{A}_{i,k} V_i u,$$

$$395 \quad = u^\top V_i^\top \sum_{k=1}^{N_i} \tilde{A}_{i,k} V_i u.$$

396

397 $\tilde{A}_{i,k}$ is an LSPSD matrix of A_i for $k = 1, \dots, N_i$. Hence, we have

$$398 \quad u^\top \sum_{j=1}^{N_{i+1}} \tilde{A}_{i+1,j} u \leq k_i u^\top V_i^\top A_i V_i u,$$

$$400 \quad \leq k_i u^\top A_{i+1} u.$$

401 We finish the proof by setting $k_{i+1} = k_i$. \square

402 **Figure 5.1** gives an illustration of the LSPSD construction provided by **Proposition 5.1**. **Figure 5.1** (top left) represents the matrix A_1 . The graph of A_1 is partitioned into 16 subdomains. Each subdomain is represented by a different color. **Figure 5.1** (top right) represents the matrix V_1 whose column vectors form a basis of the coarse space \mathcal{S}_1 . Colors of columns of V_1 correspond to those of subdomains in A_1 . **Figure 5.1** (bottom left) represents the matrix $A_2 = V_1^\top A_1 V_1$. Note that column and row indices of A_2 are associated with column indices of V_1 . Four subdomains are used at level 2. The partitioning at level 2 is related to the superdomain $\mathcal{G}_{1,j} = \llbracket 4(j-1)+1; 4(j-1)+4 \rrbracket$ for $j = 1, \dots, 4$. **Figure 5.1** (bottom right) represents an LSPSD matrix of A_2 with respect to subdomain 1 at level 2.

412 **Theorem 5.2** shows that the third condition of the fictitious subspace lemma **Lemma 2.1** holds at level i for $i = 1, \dots, L$.

414 **THEOREM 5.2.** *Let $\tilde{A}_{i,j}$ be an LSPSD of A_i associated with subdomain j , for*
 415 *$(i, j) \in \llbracket 1; L \rrbracket \times \llbracket 1; N_i \rrbracket$. Let $\tau_i > 0$, $Z_{i,j}$ be the subspace associated with $\tilde{A}_{i,j}$, and*
 416 *$P_{i,j}$ be the projection on $Z_{i,j}$ as defined in **Lemma 2.5**. Let $u_i \in \mathbb{R}^{n_i}$ and let $u_{i,j} =$*
 417 *$(D_{i,j} (I_{n_{i,j}} - P_{i,j}) R_{i,j} u_i)$ for $(i, j) \in \llbracket 1; L \rrbracket \times \llbracket 1; N_i \rrbracket$. Let $u_{i,0}$ be defined as,*

$$418 \quad u_{i,0} = (V_i^\top V_i)^{-1} V_i^\top \left(\sum_{j=1}^{N_i} R_{i,j}^\top D_{i,j} P_{i,j} R_{i,j} u_i \right).$$

419 Let $m_i = (2 + (2k_{i,c} + 1)k_i \tau_i)^{-1}$. Then,

$$420 \quad u_i = \sum_{j=0}^{N_i} R_{i,j}^\top u_{i,j},$$

421 and

$$422 \quad (5.1) \quad m_i \sum_{j=0}^{N_i} u_{i,j}^\top R_{i,j} A_i R_{i,j}^\top u_{i,j} \leq u_i^\top A_i u_i.$$

423 *Proof.* We have

$$424 \quad \sum_{j=0}^{N_i} R_{i,j}^\top u_{i,j} = V_i (V_i^\top V_i)^{-1} V_i^\top \left(\sum_{j=1}^{N_i} R_{i,j}^\top D_{i,j} P_{i,j} R_{i,j} u_i \right) + \sum_{j=1}^{N_i} R_{i,j}^\top u_{i,j}$$

425

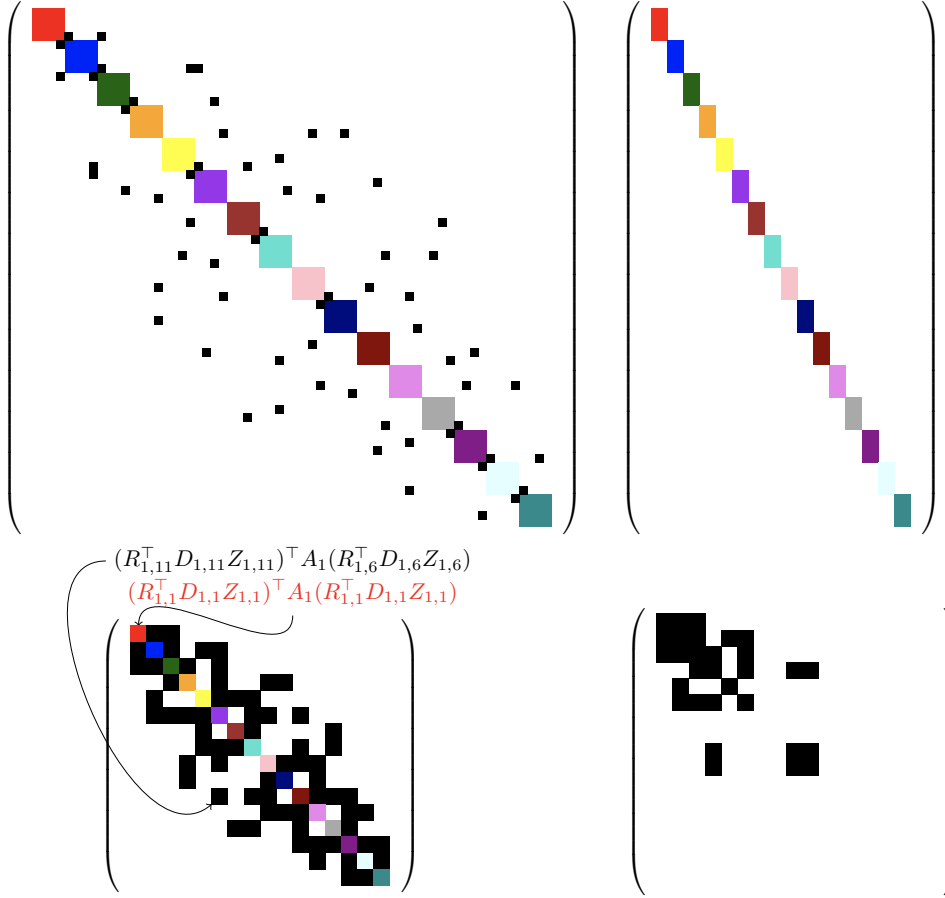


FIG. 5.1. Illustration of the LSPSD construction provided by Proposition 5.1. Top left: the matrix A_1 , top right: V_1 , bottom left: the matrix $A_2 = V_1^\top A_1 V_1$, bottom right: $\hat{A}_{2,1} = \sum_{j \in \mathcal{G}_{1,1}} V_1^\top \hat{A}_{1,j} V_1$, where $\mathcal{G}_{1,1} = 1, \dots, 4$

426 Since for all $y \in \mathcal{S}_i$, $V_i (V_i^\top V_i)^{-1} V_i^\top y = y$, we have

$$\begin{aligned}
 427 \quad \sum_{j=0}^{N_i} R_{i,j}^\top u_{i,j} &= \sum_{j=1}^{N_i} R_{i,j}^\top D_{i,j} P_{i,j} R_{i,j} u_i + \sum_{j=1}^{N_i} R_{i,j}^\top (D_{i,j} (I_{n_{i,j}} - P_{i,j}) R_{i,j} u_i), \\
 428 \quad &= \sum_{j=1}^{N_i} R_{i,j}^\top D_{i,j} R_{i,j} u_i, \\
 430 \quad &= u_i.
 \end{aligned}$$

431 To prove the inequality (5.1), we start with the inequality from Lemma 2.4. We
 432 have

$$433 \quad (5.2) \quad \sum_{j=0}^{N_i} u_{i,j}^\top R_{i,j} A_i R_{i,j}^\top u_{i,j} \leq 2u_i^\top A_i u_i + (2k_{i,c} + 1) \sum_{j=1}^{N_i} u_{i,j}^\top R_{i,j} A_i R_{i,j}^\top u_{i,j},$$

435 where we chose $u_{\mathcal{B}_i}$ in Lemma 2.4 to be $(u_{i,j})_{j=0, \dots, N_i}$ and $u_{A_i} = u_i$. In Definition 3.2,

436 we defined $Z_{i,j}$, such that for all $w \in \mathbb{R}^{n_{i,j}}$ we have

$$437 \quad ((I_{n_{i,j}} - P_{i,j})w)^\top (D_{i,j}R_{i,j}A_iR_{i,j}^\top D_{i,j}) ((I_{n_{i,j}} - P_{i,j})w) \leq \tau_i w^\top (R_{i,j}\tilde{A}_{i,j}R_{i,j}^\top) w.$$

439 Hence, in the special case $w = R_{i,j}u_i$, we can write

$$440 \quad ((I_{n_{i,j}} - P_{i,j})R_{i,j}u_i)^\top (D_{i,j}R_{i,j}A_iR_{i,j}^\top D_{i,j}) ((I_{n_{i,j}} - P_{i,j})R_{i,j}u_i) \\ 441 \quad \leq \tau_i (R_{i,j}u_i)^\top (R_{i,j}\tilde{A}_{i,j}R_{i,j}^\top) (R_{i,j}u_i).$$

444 Equivalently,

$$445 \quad u_{i,j}^\top R_{i,j}A_iR_{i,j}^\top u_{i,j} \leq \tau_i (R_{i,j}u_i)^\top R_{i,j}\tilde{A}_{i,j}R_{i,j}^\top (R_{i,j}u_i).$$

447 Plugging this inequality in (5.2) gives

$$448 \quad \sum_{j=0}^{N_i} u_{i,j}^\top R_{i,j}A_iR_{i,j}^\top u_{i,j} \leq 2u_i^\top A_i u_i + (2k_{i,c} + 1) \tau_i \sum_{j=1}^{N_i} (R_{i,j}u_i)^\top R_{i,j}\tilde{A}_{i,j}R_{i,j}^\top (R_{i,j}u_i).$$

450 Since $\tilde{A}_{i,j}$ is local, we have

$$451 \quad (R_{i,j}u_i)^\top R_{i,j}\tilde{A}_{i,j}R_{i,j}^\top (R_{i,j}u_i) = u_i^\top \tilde{A}_{i,j}u_i, \text{ for } j = 1, \dots, N_i.$$

452 By using the fact that $\tilde{A}_{i,j}$ is LSPSD of A_i for $j = 1, \dots, N_i$, we obtain the following:

$$453 \quad \sum_{j=0}^{N_i} u_{i,j}^\top R_{i,j}A_iR_{i,j}^\top u_{i,j} \leq 2u_i^\top A_i u_i + (2k_{i,c} + 1) k_i \tau_i u_i^\top A_i u_i.$$

455 Multiplying both sides with m_i ends the proof, i.e.,

$$456 \quad m_i \sum_{j=0}^{N_i} u_{i,j}^\top R_{i,j}A_iR_{i,j}^\top u_{i,j} \leq u_i^\top A_i u_i. \quad \square$$

458 In [3], the authors presented the minimal subspace that replaces $Z_{i,j}$ (defined in (3.3)
459 and used in Theorem 5.2) that is required to prove Theorem 5.2. The main difference
460 with respect to the subspace that we define in (3.3) is that it is not necessary to include
461 the entire kernel of the LSPSD matrix, $K_{i,j}$, in $Z_{i,j}$, see Definition 3.2. Nevertheless,
462 in this work, we include the entire kernel of the LSPSD matrix in the definition of
463 $Z_{i,j}$. This allows us to ensure that the kernels of Neumann matrices are transferred
464 across the levels, see Theorem 5.4. And in addition, this corresponds to the definition
465 used in GenEO [12, Lemma 7.7] and to its implementation in the HPDDM library
466 [19].

467 Theorem 5.3 provides an upper bound on the condition number of the preconditioned
468 matrix $M_i^{-1}A_i$ for $i = 1, \dots, L$.

469 THEOREM 5.3. *Let M_i be the additive Schwarz preconditioner at level i combined
470 with the coarse space correction induced by \mathcal{S}_i defined in (3.4). The following inequality
471 holds,*

$$472 \quad \kappa(M_i^{-1}A_i) \leq (k_{i,c} + 1) (2 + (2k_{i,c} + 1)k_i\tau_i).$$

473 *Proof.* Lemma 2.2, Lemma 2.3, and Theorem 5.2 prove that the multilevel preconditioner verifies the conditions in Lemma 2.1 at each level i . Hence, the spectrum of the preconditioned matrix $M_i^{-1}A_i$ is contained in the interval $[(2 + (2k_{i,c} + 1)k_i\tau_i)^{-1}, k_{i,c} + 1]$. Equivalently, the condition number of the preconditioned matrix at level i verifies the following inequality

$$478 \quad \kappa(M_i^{-1}A_i) \leq (k_{i,c} + 1)(2 + (2k_{i,c} + 1)k_i\tau_i). \quad \square$$

479 Proposition 5.1 shows that the constant k_i associated with the LSPSD matrices at level i is independent of the number of levels and bounded by the number of subdomains at level 1. Indeed,

$$482 \quad k_1 \geq k_i \text{ for } i = 2, \dots, L.$$

483 Furthermore, in the case where the LSPSD matrices at the first level are the Neumann matrices, k_i is bounded by the maximum number of subdomains at level 1 that share an unknown.

484 The constant $k_{i,c}$ for $i = 1, \dots, L$ is the minimum number of distinct colors so that $\{span\{R_{i,j}^\top\}\}_{1 \leq j \leq N_i}$ of the same color are mutually A_i -orthogonal. Both constants k_i and $k_{i,c}$ are independent of the number of subdomains for each level i .

485 The constant τ_i can be chosen such that the condition number of the preconditioned system at level i is upper bounded by a prescribed value. Hence, this allows to have a robust convergence of the preconditioned Krylov solver at each level.

486 Algorithm 5.1 presents the construction of the multilevel additive Schwarz method by using GenEO. The algorithm iterates over the levels. At each level, three main operations are performed. First, the construction of the LSPSD matrices. At level 1, the LSPSD matrices are the Neumann matrices, otherwise, Proposition 5.1 is used to compute them. Once the LSPSD matrix is available, the generalized eigenvalue problem in (3.2) has to be solved concurrently. Given the prescribed upper bound on the condition number, $Z_{i,j}$ can be set. Finally, the coarse space is available and the coarse matrix is assembled.

487 The following Theorem 5.4, describes how the kernel of Neumann matrices are transferred across the levels.

488 THEOREM 5.4. *Suppose that $\tilde{A}_{1,j}$ is the Neumann matrix associated with the subdomain $\Omega_{1,j}$ for $j \in \llbracket 1; N_1 \rrbracket$. For $(i, j) \in \llbracket 2; L \rrbracket \times \llbracket 1; N_i \rrbracket$, let*

- 489 • $\tilde{A}_{i,j}$ be the LSPSD matrices associated with $A_{i,j}$ defined in Proposition 5.1,
- 490 • $\mathcal{G}_{i-1,j}$ be the corresponding superdomains,
- 491 • $\mathcal{G}_{i-1,j}^1$ be the union of subdomains at level 1 which contribute hierarchically to obtain $\mathcal{G}_{i-1,j}$,
- 492 • $\tilde{A}_{\mathcal{G}_{i-1,j}}$ be the Neumann matrix associated with $\mathcal{G}_{i-1,j}^1$ (seeing $\mathcal{G}_{i-1,j}^1$ as a subdomain),
- 493 • $A_{\mathcal{G}_{i-1,j}}$ be the restriction of A to the subdomain $\mathcal{G}_{i-1,j}^1$.

494 Then, the kernel of $\tilde{A}_{\mathcal{G}_{i-1,j}}$ is included in the kernel of $\left(\prod_{l=1}^{i-1} V_l\right) \tilde{A}_{i,j} \left(\prod_{l=1}^{i-1} V_l\right)^\top$.

495 *Proof.* First, note that for any LSPSD matrix computed as in Proposition 5.1, we have

$$\left(\prod_{l=1}^{i-1} V_l\right) \tilde{A}_{i,j} \left(\prod_{l=1}^{i-1} V_l\right)^\top = \left(\prod_{l=1}^{i-1} V_l\right) \left(\prod_{l=1}^{i-1} V_l\right)^\top \sum_{k \in \mathcal{G}_{i,j}^1} \tilde{A}_{1,k} \left(\prod_{l=1}^{i-1} V_l\right) \left(\prod_{l=1}^{i-1} V_l\right)^\top.$$

Algorithm 5.1 Multilevel GenEO

Require: $A_1 = A \in \mathbb{R}^{n \times n}$ SPD, $L + 1$ number of levels, N_i number of subdomains at each level, $\mathcal{G}_{i,j}$ sets of superdomains

Ensure: preconditioner at each level i , M_i^{-1} with bounded condition number of $M_i^{-1}A_i$

- 1: **for** $i = 1, \dots, L$ **do**
- 2: **for** each subdomain $j = 1, \dots, N_i$ **do**
- 3: $A_{i,j} = R_{i,j}A_iR_{i,j}^\top$ (local matrix associated with subdomain j)
- 4: **if** $i = 1$ **then**
- 5: local SPSD $\tilde{A}_{i,j}$ is Neumann matrix of subdomain j
- 6: **else**
- 7: compute local SPSD matrix as

$$\tilde{A}_{i,j} = \sum_{k \in \mathcal{G}_{i,j}} V_{i-1}^\top \tilde{A}_{i-1,k} V_{i-1}$$

- 8: **end if**
- 9: solve the generalized eigenvalue problem (3.2), set $Z_{i,j}$ as in (3.3)
- 10: **end for**
- 11: $S_i = \bigoplus_{j=1}^{N_i} D_{i,j}R_{i,j}^\top Z_{i,j}$, V_i basis of S_i
- 12: coarse matrix $A_{i+1} = V_i^\top A_i V_i$, $A_{i+1} \in \mathbb{R}^{n_{i+1} \times n_{i+1}}$
- 13: **end for**
- 14: $M_i^{-1} = V_i A_{i+1}^{-1} V_i^\top + \sum_{j=1}^{N_i} R_{i,j}^\top A_{i,j}^{-1} R_{i,j}$

Moreover, due to the fact that $\tilde{A}_{\mathcal{G}_{i-1,j}}$ and $\tilde{A}_{1,k}$ are Neumann matrices, we have

$$u^\top \tilde{A}_{\mathcal{G}_{i-1,j}} u \leq u^\top \sum_{k \in \mathcal{G}_{i,j}^1} \tilde{A}_{1,k} u \leq k_1 u^\top \tilde{A}_{\mathcal{G}_{i-1,j}} u.$$

512 On one hand, the kernels of $\tilde{A}_{1,k}$ for $k \in \mathcal{G}_{i,j}^1$ are included, by construction, in the image
 513 of V_1 , see Definition 3.2. So is their intersection which is the kernel of $\sum_{k \in \mathcal{G}_{i,j}^1} \tilde{A}_{1,k}$.

514 On the other hand, the previous two-sided inequality implies that the kernels of $\tilde{A}_{\mathcal{G}_{i-1,j}}$
 515 and $\sum_{k \in \mathcal{G}_{i,j}^1} \tilde{A}_{1,k}$ are identical. Hence, the kernel of $\tilde{A}_{\mathcal{G}_{i-1,j}}$ is included in the image
 516 of QQ^\top , where $Q = \left(\prod_{l=1}^{i-1} V_l\right)$. \square

517 **Theorem 5.4** proves that the kernel of the Neumann matrix of a union of subdomains
 518 at level 1 that hierarchically contribute to form a subdomain at level i is conserved by
 519 the construction of the hierarchical coarse spaces. For example in the case of linear
 520 elasticity, it is essential to include the rigid body motions in the coarse space in order
 521 to have a fast convergence. As these are included in the kernel of the Neumann matrix
 522 of the subdomain, the hierarchical coarse space includes them, consequently.

523 **6. Numerical experiments.** In this section, the developed theory is validated
 524 numerically with FreeFEM [14] for finite element discretizations and HPDDM [19]
 525 for domain decomposition methods. We present numerical experiments on two highly
 526 challenging problems illustrating the efficiency and practical usage of the proposed
 527 method. For both problems, we use $N_1 = 2,048$ MPI processes (equal to the number
 528 of subdomains at level 1), and the domain partitioning is performed using ParMETIS

529 [22], with no control on the alignments of subdomain interfaces. We compare the
 530 two-level GenEO preconditioner and its multilevel extension by varying N_2 between 4
 531 and 256. For the two-level method, N_2 corresponds to the number of MPI processes
 532 that solve the coarse problem in a distributed fashion using MKL CPARDISO [17].
 533 For the multilevel method, N_3 is set to 1, i.e., a three-level method is used. The goal
 534 of these numerical experiments is to show that when one switches from a two-level
 535 method with an exact coarse solver, to our proposed multilevel method, the number
 536 of outer iterations is not impacted. Thus, three levels are sufficient. As an outer
 537 solver, since all levels but the coarsest are solved approximately, the flexible GMRES
 538 [31] is used. It is stopped when relative unpreconditioned residuals are lower than
 539 10^{-6} . Subdomain matrices $\{A_{i,j}\}_{1 \leq i \leq 2, 1 \leq j \leq N_i}$ are factorized concurrently using MKL
 540 PARDISO, and eigenvalue problems are solved using ARPACK [24]. In both, two-
 541 and three-level GenEO, we factorize the local matrices $A_{1,j}$ for $j \in \llbracket 1; N_1 \rrbracket$ and solve
 542 the generalized eigenvalue problems concurrently at the first level. For this reason,
 543 we do not take into account the time needed for these two steps which are performed
 544 without any communication between MPI processes. We compare the time needed
 545 to assemble and factorize A_2 in the two-level approach against the time needed to
 546 assemble A_2 and local SPSD matrices $\tilde{A}_{2,j}$ for $j \in \llbracket 1; N_2 \rrbracket$, solve the generalized
 547 eigenvalue problems concurrently on the second level, assemble, and factorize the
 548 matrix A_3 in the three-level approach. We also compare the time spent in the outer
 549 Krylov solver during the solution phase. Readers interested by a comparison of the
 550 efficiency of GenEO and multigrid methods such as GAMG [1] are referred to [18].
 551 FreeFEM scripts used to produce the following results are available at the following
 552 URL: <https://github.com/prj-/aldaas2019multi>¹.

553 **6.1. Diffusion test cases.** The scalar diffusion equation with highly heteroge-
 554 neous coefficient κ is solved in $[0, 1]^d$ ($d = 2$ or 3). The strong formulation of the
 555 equation is:

$$\begin{aligned}
 & -\nabla \cdot (\kappa \nabla u) = 1 \quad \text{in } \Omega, \\
 & u = 0 \quad \text{on } \Gamma_D, \\
 & \frac{\partial u}{\partial n} = 0 \quad \text{on } \Gamma_N.
 \end{aligned}$$

558 The exterior normal vector to the boundary of Ω is denoted n . Γ_D is the subset
 559 of the boundary of Ω corresponding to $x = 0$ in 2D and 3D. Γ_N is defined as the
 560 complementary of Γ_D with respect to the boundary of Ω . We discretize the equation
 561 using \mathbb{P}_2 and \mathbb{P}_4 finite elements in the 3D and 2D test cases, respectively. The number
 562 of unknowns is 441×10^6 and 784×10^6 , with approximately 28 and 24 nonzero
 563 elements per row in the 3D and 2D cases, respectively. The heterogeneity is due
 564 to the jumps in the diffusion coefficient κ , see Figure 6.1, which is modeled using
 565 a combination of jumps and channels, cf. the file `coefficients.idp` from <https://github.com/prj-/aldaas2019multi>.

567 The results in two dimensions are reported in Table 6.1. The number of outer
 568 iterations for both two- and three-level GenEO is 32. The size of the level 2 operator
 569 is $n_2 = 25 \times 2,048 = 51,200$. In all numerical results, the number of eigenvectors per
 570 subdomain, here 25, is fixed. This is because ARPACK cannot a priori compute all
 571 eigenpairs below a certain threshold, and an upper bound has to be provided instead.

¹note to reviewers: the repository is now public

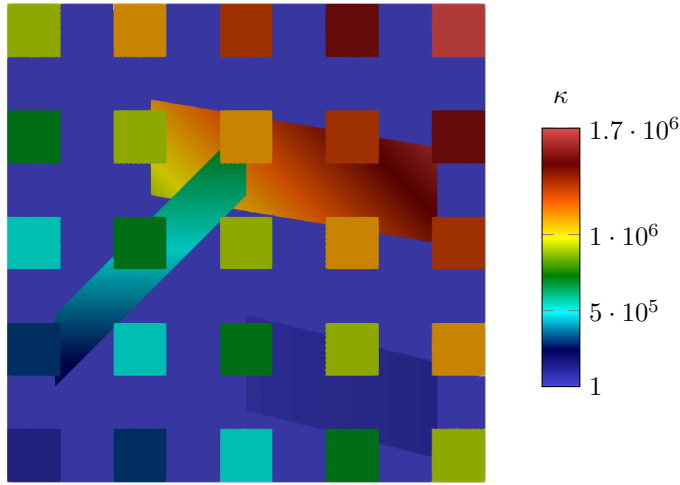


FIG. 6.1. Variation of the coefficient κ used for the diffusion test case

572 HPDDM is capable of filtering the eigenpairs for which eigenvalues are above the user-
 573 specified GenEO threshold from [Lemma 2.5](#). However, this means that the coarse
 574 operator may be unevenly distributed. With a fixed number of eigenvectors per sub-
 575 domain, it is possible to use highly optimized uniform MPI routines and block matrix
 576 formats. Hence, for performance reasons, all eigenvectors computed by ARPACK are
 577 kept when building coarse operators. It is striking that the multilevel method does not
 578 deteriorate the numerical performance of the outer solver. For the two-level method,
 579 the first column corresponds to the time needed to assemble the Galerkin operator A_2
 580 from [\(3.5\)](#) (assuming V_1 has already been computed by ARPACK), and to factorize it
 581 using N_2 MPI processes. For the three-level method, the first column corresponds to
 582 the time needed to assemble level 2 local subdomain matrices $\{A_{2,j}\}_{1 \leq j \leq N_2}$, level 2
 583 local SPSD matrices, solve the generalized eigenvalue problem [\(3.2\)](#) concurrently, as-
 584 semble the Galerkin operator A_3 and factorize it on a single process. The size of
 585 the level 3 operator is $n_3 = 20 \times N_2$. For both two- and three-level methods, the
 586 second column is the time spent in the outer Krylov solver once the preconditioner
 587 has been set up. In the last column of the three-level method, the number of inner
 588 iterations for solving systems involving A_2 , which is not inverted exactly anymore,
 589 is reported. For all tables, this column is an average over all successive outer itera-
 590 tions. Another important numerical property of our method is that, thanks to fully
 591 controlled bounds at each level, the number of inner iterations is low, independently
 592 of the number of superdomains N_2 . Because this problem is not large enough, it is
 593 still tractable by a two-level method, for which HPDDM was highly optimized for.
 594 Thus, there is no performance gain to be expected at this scale. However, one can
 595 notice that the construction of the coarse operator(s) scales nicely with N_2 for the
 596 three-level method, whereas the performance of the direct solver MKL CPARDISO
 597 quickly stagnates because of the finer and finer parallel workload granularity.

598 The results in three dimensions are reported in [Table 6.2](#). The number of outer
 599 iterations for both the two- and three-level GenEO is 19. The observations made
 600 in two dimensions still hold, and the dimensions of A_2 and A_3 are the same. Once
 601 again, it is important to note that the number of outer iterations is the same for both
 602 methods.

N_2	two-level GenEO			three-level GenEO			
	CS	solve	% of nnz A_2	CS	solve	inner it.	% of nnz A_3
4	2.4	11.9	0.19	6.5	27.4	14	56.0
16	1.8	11.3		3.6	15.4	15	19.0
64	1.9	12.1		3.0	16.7	14	5.5
256	2.4	18.4		2.8	13.9	13	1.4

TABLE 6.1
 Diffusion 2D test case, comparison between two- and three-level GenEO. The percentage of nonzero entries in A_1 is 0.3%.

N_2	two-level GenEO			three-level GenEO			
	CS	solve	% of nnz A_2	CS	solve	inner it.	% of nnz A_3
4	7.0	20.9	0.36	16.9	43.6	17	62.0
16	5.0	19.8		7.7	26.7	17	28.0
64	5.1	20.1		5.8	32.7	15	8.9
256	5.2	24.1		5.3	22.6	14	2.6

TABLE 6.2
 Diffusion 3D test case, comparison between two- and three-level GenEO. The percentage of nonzero entries in A_1 is 0.5%.

603 **6.2. Linear elasticity test cases.** The system of linear elasticity with highly
 604 heterogeneous elastic moduli is solved in 2D and 3D. The strong formulation of the
 605 equation is given as:

$$\begin{aligned}
 (6.1) \quad & \operatorname{div} \sigma(u) + f = 0 \quad \text{in } \Omega, \\
 & u = 0 \quad \text{on } \Gamma_D, \\
 & \sigma(u) \cdot n = 0 \quad \text{on } \Gamma_N.
 \end{aligned}$$

608 The physical domain Ω is a beam of dimensions $[0, 10] \times [0, 1]$, extruded for $z \in$
 609 $[0, 1]$ in 3D. The Cauchy stress tensor $\sigma(\cdot)$ is given by Hooke's law: it can be expressed
 610 in terms of Young's modulus E and Poisson's ratio ν .

$$\sigma_{ij}(u) = \begin{cases} 2\mu\varepsilon_{ij}(u) & i \neq j, \\ 2\mu\varepsilon_{ii}(u) + \lambda\operatorname{div}(u) & i = j, \end{cases}$$

612 where

$$\varepsilon_{ij}(u) = \frac{1}{2} \left(\frac{\partial u_i}{\partial x_j} + \frac{\partial u_j}{\partial x_i} \right), \mu = \frac{E}{2(1+\nu)}, \text{ and } \lambda = \frac{E\nu}{1-2\nu}.$$

614 The exterior normal vector to the boundary of Ω is denoted n . Γ_D is the subset
 615 of the boundary of Ω corresponding to $x = 0$ in 2D and 3D. Γ_N is defined as the
 616 complementary of Γ_D with respect to the boundary of Ω . We discretize (6.1) using
 617 the following vectorial finite elements: $(\mathbb{P}_2, \mathbb{P}_2, \mathbb{P}_2)$ in 3D and $(\mathbb{P}_3, \mathbb{P}_3)$ in 2D. The
 618 number of unknowns is 146×10^6 and 847×10^6 , with approximately 82 and 34
 619 nonzero elements per row in the 3D and 2D cases, respectively. The heterogeneity is
 620 due to the jumps in E and ν . We consider discontinuous piecewise constant values
 621 for E and ν : $(E_1, \nu_1) = (2 \times 10^{11}, 0.25)$, $(E_2, \nu_2) = (10^7, 0.45)$, see Figure 6.2.

622 Results in two (resp. three) dimensions are reported in Table 6.3 (resp. Table 6.4).
 623 The number of outer iterations are 73 and 45 respectively. For these test cases, we

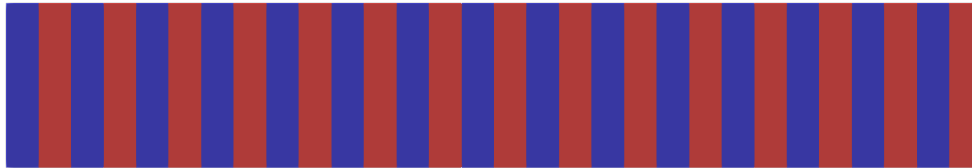


FIG. 6.2. Variation of the structure coefficients used for the elasticity test case

N_2	two-level GenEO			three-level GenEO			
	CS	solve	% of nnz A_2	CS	solve	inner it.	% of nnz A_3
4	4.8	52.7	0.18	22.5	179.3	31	43.0
16	3.9	50.3		9.3	124.9	57	17.0
64	4.0	53.1		7.2	71.5	34	4.9
256	4.8	63.2		6.8	71.2	44	1.4

TABLE 6.3
Elasticity 2D test case, comparison between two- and three-level GenEO. The percentage of nonzero entries in A_1 is 0.4%.

624 slightly relaxed the criterion for selecting eigenvectors in coarse spaces, which explains
 625 why the iteration counts increase. However, the same observations as for the diffusion
 626 test cases still hold. The dimension of the level 2 matrix is $n_2 = 50 \times 2,048 = 1.02 \cdot 10^5$,
 627 while for the level 3 matrix it is $n_3 = 20 \times N_2$. This means that 50 (resp. 20)
 628 eigenvectors are kept per level 1 (resp. level 2) subdomains. We observe that the
 629 number of iterations of the inner solver increases slowly when increasing the number
 630 of subdomains from 4 to 256 in the 2D case and remains almost constant in the 3D
 631 case. In terms of runtime, the two-level GenEO is faster than three-level GenEO for
 632 these matrices of medium dimensions.

633 To show the potential of our method at larger scales, a three-dimensional linear
 634 elasticity problem of size 593×10^6 is now solved on $N_1 = 16,384$ processes and
 635 $N_2 = 256$ superdomains. With the two-level method, A_2 is assembled and factorized
 636 in 40.8 seconds. With the three-level method, this step now takes 35.1 seconds, see
 637 Table 6.5. There is a two iterations difference in the iteration count. Not taking
 638 into account the preconditioner setup, the problem is solved in 222.5 seconds in the
 639 two-level case and 90.1 seconds in the multilevel case. In this test case the cost of
 640 applying the two-level preconditioner on a given vector is approximately twice the cost
 641 of applying the multilevel variant. At this regime, it is clear that there are important
 642 gains for the solution phase. At even greater scales, gains for the setup phase are
 643 also expected. Moreover, another interesting fact to note regarding computation time
 644 is that the generalized eigenvalue problems solved concurrently at the first level to
 645 obtain V_1 actually represents a significant part of the total time of 377.6 seconds (resp.
 646 244.8 seconds) with the two- (resp. three-)level method: 78.2 seconds. This cost can
 647 be reduced by taking a larger number of (smaller) subdomains, with the drawback of
 648 increasing the size of V_1 and thus A_2 . This drawback represents a clear bottleneck
 649 for the two-level method but is alleviated by using the three-level method, making it
 650 a good candidate for problems at greater scales.

651 **7. Conclusion.** In this paper, we reviewed general properties of overlapping
 652 Schwarz preconditioners and presented a framework for its multilevel extension. We

N_2	two-level GenEO			three-level GenEO			
	CS	solve	% of nnz A_2	CS	solve	inner it.	% of nnz A_3
4	28.5	46.9	0.38	78.9	296.7	23	43.0
16	17.3	35.4		24.5	124.5	23	19.0
64	15.0	33.2		15.4	62.2	21	7.9
256	13.6	40.7		10.6	50.7	23	2.5

TABLE 6.4
Elasticity 3D test case, comparison between two- and three-level GenEO. The percentage of nonzero entries in A_1 is 3.3%.

N_2	two-level GenEO		three-level GenEO		
	CS	solve	CS	solve	inner it.
256	40.8	222.5	35.1	90.1	11

TABLE 6.5
Elasticity 3D test case, comparison between two- and three-level GenEO

653 generalized the local SPSD splitting presented in [3] to cover a larger set of matrices
 654 leading to more flexibility for building robust coarse spaces. Based on local SPSD
 655 matrices on the first level, we presented how to compute local SPSD matrices for
 656 coarser levels. The multilevel solver based on hierarchical local SPSD matrices is
 657 robust and guarantees a bound on the condition number of the preconditioned matrix
 658 at each level depending on predefined values. Numerical experiments illustrate the
 659 theory and prove the efficiency of the method on challenging problems of large size
 660 arising from heterogeneous linear elasticity and diffusion problems with jumps in the
 661 coefficients of multiple orders of magnitude.

662 **8. Acknowledgments.** We would like to thank the anonymous referees for their
 663 comments and remarks that helped us improve the clarity of this manuscript. This
 664 work was granted access to the HPC resources of TGCC@CEA under the allocation
 665 A0050607519 made by GENCI. The work of the second author was supported by the
 666 NLAFFET project as part of European Union’s Horizon 2020 research and innovation
 667 program under grant 671633.

668 REFERENCES

669 [1] M. F. ADAMS, H. H. BAYRAKTAR, T. M. KEAVENY, AND P. PAPADOPOULOS, *Ultrascaleable*
 670 *Implicit Finite Element Analyses in Solid Mechanics with over a Half a Billion Degrees of*
 671 *Freedom*, in Proceedings of the 2004 ACM/IEEE Conference on Supercomputing, SC '04,
 672 IEEE Computer Society, 2004.
 673 [2] M. F. ADAMS AND J. W. DEMMEL, *Parallel Multigrid Solver for 3D Unstructured Finite El-*
 674 *ement Problems*, in Proceedings of the 1999 ACM/IEEE Conference on Supercomputing,
 675 SC '99, ACM, 1999.
 676 [3] H. AL DAAS AND L. GRIGORI, *A class of efficient locally constructed preconditioners based on*
 677 *coarse spaces*, SIAM Journal on Matrix Analysis and Applications, 40 (2019), pp. 66–91.
 678 [4] S. BADIA, A. MARTÍN, AND J. PRINCIPE, *Multilevel balancing domain decomposition at extreme*
 679 *scales*, SIAM Journal on Scientific Computing, 38 (2016), pp. C22–C52.
 680 [5] P. E. BJØRSTAD, M. J. GANDER, A. LONELAND, AND T. RAHMAN, *Does SHERM for Additive*
 681 *Schwarz Work Better than Predicted by Its Condition Number Estimate?*, in International
 682 Conference on Domain Decomposition Methods, Springer, 2017, pp. 129–137.
 683 [6] A. BORZI, V. DE SIMONE, AND D. DI SERAFINO, *Parallel algebraic multilevel Schwarz pre-*
 684 *conditioners for a class of elliptic PDE systems*, Computing and Visualization in Science, 16
 685 (2013), pp. 1–14.

- 686 [7] M. BREZINA, A. CLEARY, R. FALGOUT, V. HENSON, J. JONES, T. MANTEUFFEL, S. MCCORMICK,
687 AND J. RUGE, *Algebraic Multigrid Based on Element Interpolation (AMGe)*, SIAM Journal
688 on Scientific Computing, 22 (2001), pp. 1570–1592.
- 689 [8] X.-C. CAI AND M. SARKIS, *A restricted additive Schwarz preconditioner for general sparse*
690 *linear systems*, SIAM Journal on Scientific Computing, 21 (1999), pp. 792–797.
- 691 [9] T. F. CHAN AND T. P. MATHEW, *Domain decomposition algorithms*, Acta Numerica, 3 (1994),
692 pp. 61–143.
- 693 [10] T. CHARTIER, R. D. FALGOUT, V. E. HENSON, J. JONES, T. MANTEUFFEL, S. MCCORMICK,
694 J. RUGE, AND P. S. VASSILEVSKI, *Spectral AMGe (ρ AMGe)*, SIAM Journal on Scientific
695 Computing, 25 (2003), pp. 1–26.
- 696 [11] C. CHEVALIER AND F. PELLEGRINI, *PT-SCOTCH: A tool for efficient parallel graph ordering*,
697 Parallel Computing, 34 (2008), pp. 318–331. Parallel Matrix Algorithms and Applications.
- 698 [12] V. DOLEAN, P. JOLIVET, AND F. NATAF, *An introduction to domain decomposition methods*,
699 Society for Industrial and Applied Mathematics, 2015. Algorithms, theory, and parallel
700 implementation.
- 701 [13] M. GRIEBEL AND P. OSWALD, *On the abstract theory of additive and multiplicative Schwarz*
702 *algorithms*, Numerische Mathematik, 70 (1995), pp. 163–180.
- 703 [14] F. HECHT, *New development in FreeFem++*, Journal of Numerical Mathematics, 20 (2012),
704 pp. 251–266.
- 705 [15] A. HEINLEIN, A. KLAWONN, O. RHEINBACH, AND F. RÖVER, *A Three-Level Extension of the*
706 *GDSW Overlapping Schwarz Preconditioner in Three Dimensions*, technical report, Uni-
707 versität zu Köln, November 2018.
- 708 [16] V. E. HENSON AND U. M. YANG, *BoomerAMG: A parallel algebraic multigrid solver and pre-*
709 *conditioner*, Applied Numerical Mathematics, 41 (2002), pp. 155–177. Developments and
710 Trends in Iterative Methods for Large Systems of Equations.
- 711 [17] INTEL, *MKL web page*. <https://software.intel.com/en-us/intel-mkl>, 2019.
- 712 [18] P. JOLIVET, *Domain decomposition methods. Application to high-performance computing*, the-
713 ses, Université de Grenoble, Oct. 2014.
- 714 [19] P. JOLIVET, F. HECHT, F. NATAF, AND C. PRUD’HOMME, *Scalable domain decomposition pre-*
715 *conditioners for heterogeneous elliptic problems*, in Proceedings of the International Con-
716 ference on High Performance Computing, Networking, Storage and Analysis, SC13, ACM,
717 2013.
- 718 [20] J. JONES AND P. VASSILEVSKI, *AMGe Based on Element Agglomeration*, SIAM Journal on
719 Scientific Computing, 23 (2001), pp. 109–133.
- 720 [21] D. KALCHEV, C. LEE, U. VILLA, Y. EFENDIEV, AND P. VASSILEVSKI, *Upscaling of mixed finite*
721 *element discretization problems by the spectral AMGe method*, SIAM Journal on Scientific
722 Computing, 38 (2016), pp. A2912–A2933.
- 723 [22] G. KARYPIS AND V. KUMAR, *Multilevel k-way partitioning scheme for irregular graphs*, Journal
724 of Parallel and Distributed Computing, 48 (1998), pp. 96–129.
- 725 [23] F. KONG AND X.-C. CAI, *A highly scalable multilevel Schwarz method with boundary geometry*
726 *preserving coarse spaces for 3D elasticity problems on domains with complex geometry*,
727 SIAM Journal on Scientific Computing, 38 (2016), pp. C73–C95.
- 728 [24] R. LEHOUCQ, D. SORENSEN, AND C. YANG, *ARPACK users’ guide: solution of large-scale*
729 *eigenvalue problems with implicitly restarted Arnoldi methods*, vol. 6, Society for Industrial
730 and Applied Mathematics, 1998.
- 731 [25] J. MANDEL, B. SOUSEDÍK, AND C. R. DOHRMANN, *Multispace and multilevel BDDC*, Comput-
732 ing, 83 (2008), pp. 55–85.
- 733 [26] O. MARQUES, A. DRUINSKY, X. S. LI, A. T. BARKER, P. VASSILEVSKI, AND D. KALCHEV, *Tuning*
734 *the coarse space construction in a spectral AMG solver*, Procedia Computer Science, 80
735 (2016), pp. 212–221. International Conference on Computational Science 2016, ICCS 2016,
736 6–8 June 2016, San Diego, California, USA.
- 737 [27] S. V. NEPOMNYASCHIKH, *Mesh theorems of traces, normalizations of function traces and their*
738 *inversions*, Russian Journal of Numerical Analysis and Mathematical Modelling, 6 (1991),
739 pp. 1–25.
- 740 [28] ———, *Decomposition and fictitious domains methods for elliptic boundary value problems*,
741 1992.
- 742 [29] Y. NOTAY, *An aggregation-based algebraic multigrid method*, Electronic Transactions on Nu-
743 merical Analysis, 37 (2010), pp. 123–146.
- 744 [30] C. PECHSTEIN, *Finite and boundary element tearing and interconnecting solvers for multiscale*
745 *problems*, vol. 90, Springer Science & Business Media, 2012.
- 746 [31] Y. SAAD., *A Flexible Inner–Outer Preconditioned GMRES Algorithm*, SIAM Journal on Sci-
747 entific Computing, 14 (1993), pp. 461–469.

- 748 [32] Y. SAAD, *Iterative Methods for Sparse Linear Systems*, Society for Industrial and Applied
749 Mathematics, 2nd ed., 2003.
- 750 [33] N. SPILLANE, V. DOLEAN, P. HAURET, F. NATAF, C. PECHSTEIN, AND R. SCHEICHL, *Abstract*
751 *robust coarse spaces for systems of PDEs via generalized eigenproblems in the overlaps*,
752 *Numerische Mathematik*, 126 (2014), pp. 741–770.
- 753 [34] J. TOIVANEN, P. AVERY, AND C. FARHAT, *A multilevel feti-dp method and its performance for*
754 *problems with billions of degrees of freedom*, *International Journal for Numerical Methods*
755 *in Engineering*, 116 (2018), pp. 661–682.
- 756 [35] A. TOSELLI AND O. WIDLUND, *Domain Decomposition Methods - Algorithms and Theory*,
757 Springer Series in Computational Mathematics, Springer Berlin Heidelberg, 2005.
- 758 [36] J. XU, *Theory of Multilevel Methods*, PhD thesis, Cornell University, 1989.
- 759 [37] S. ZAMPINI, *PCBDDC: A class of robust dual-primal methods in PETSc*, *SIAM Journal on*
760 *Scientific Computing*, 38 (2016), pp. S282–S306.